SEMARAK ILMU PUBLISHING

Semarak Current Biomedical Technology Research Journal

Journal homepage:
https://semarakilmu.com.my/journals/index.php/scbrj/index
ISSN: XXX-XXX

Analytical Simulation of Magnetohydrodynamics Casson Blood Flow using Carbon Nanotubes in a Channel with Atherosclerosis Condition

Wan Nura'in Nabilah Noranuar[1], Ahmad Qushairi Mohamad[1,*], Lim Yeou Jiann[1], Sharidan Shafie[1]

[1] Department of Mathematical Sciences, Faculty of Science, Universiti Teknologi Malaysia, 81310 Skudai, Johor, Malaysia

ARTICLE INFO

Article history:
Received 29 March 2024
Received in revised form 9 May 2024
Accepted 20 May 2024
Available online 31 May 2024

Keywords:
Blood flow; carbon nanotubes; Laplace transformations; channel; Casson fluid

ABSTRACT

Atherosclerosis is a condition where the arteries become narrowed and hardened due to the buildup of plaque, which is made up of cholesterol, fat and other substances. This narrowing restricts blood flow and can lead to severe complications such as heart attacks and strokes. The biofluid dynamics of blood is commonly studied numerically using various numerical methods, which can lead to the inaccuracies of results. Therefore, the analytical solution is important as it can provide a verification to the approximate solutions obtained by numerical methods. The present study interested to discover the realm of blood rheology in analytical field by investigating the blood flow under the influences of nanoparticles (drug-carriers), porosity (plaque) and magnetic field (external source of energy). The Navier Stokes equations incorporating the Casson fluid model govern the fluid flow subjected to suitable initial and boundary conditions. The conversion of dimensional governing equations into dimensionless is conducted using relevant dimensionless variables, which are then employed by the Laplace transform to attain the analytical solutions. The results report that the addition of carbon nanotube (CNTs) significantly enhances the heat transfer and velocity of the blood, which can be an advantage in the process of plaque fragmentation. Besides, this analytical study of blood flow provides valuable theoretical insights into the fundamental principles governing cardiovascular physiology, guiding the development of medical devices and treatments and informing clinical decision-making.

1. Introduction

Numerous cardiovascular conditions, notably atherosclerosis, have been identified as leading causes of fatalities in both developed and developing nations. Investigating blood flow within a narrowed artery is crucial as it sheds light on the dynamics of blood circulation and the mechanical properties of vessel walls, both of which contribute to various cardiovascular ailments [1-3]. Many researchers [4-6] have focused on analyzing the pulsatile flow of blood in arteries afflicted with single mild stenosis. While in other studies [7-9], multiple stenosis are frequently affect in the femoral and pulmonary arteries, by which the existence of overlapping stenosis exacerbates the blood flow issue. The examination of blood rheology and flow serves several aims, encompassing not only comprehending aspects of health and disease but also fundamentally discerning the nature of this

* *Corresponding author.*
E-mail address: ahmadqushairi@utm.my

fluid model [10-12]. Featuring the characteristic of blood flow through a large diameter of blood vessels at a high shear rate with mild stenosis, a few researchers treated this fluid as the Newtonian fluid [13-15]. It is however not valid, when the flow in smaller arteries and downstream of the stenosis is low, as well as when the shear rate is low. It has been noted that blood demonstrates notable non-Newtonian characteristics in certain pathological situations. Mandal [16] used a generalized Power-law model to characterize the unsteady non-linear blood flow through numerical investigation. The results were compared with a visco-elastic wall and an elastic (moving) vascular wall. Wang *et al.,* [17] studied the Maxwell fluid model for blood flow under the influences of pulsatile pressure gradient, magnetic field and radiative heat transfer.

Due to its significance in biological and commercial applications, laminar flow and heat transfer in channels/pipes with different cross sections have attracted a lot of attention in recent years. According to Abu-Hamdeh *et al.,* [18] and [19], the geometry of a channel is often used to represent blood vessels because it provides a simplified yet accurate model for understanding blood flow dynamics, making them easier to analyze mathematically. Ali *et al.,* [20] characterized the blood flow by Casson fluid model and investigated numerically the flow of blood in porous channel. Tanveer *et al.,* [21] studied the heat and mass transfer of chemically reacting blood flow in a flexible channel subjected to Bingham fluid model. The impact of solute dispersion on the Casson blood flow moving through channel with external body acceleration was analyzed by [22]. Zaman and Khan [23] used the Carreau fluid model in channel to formulate their investigation on the shear thickening and shear thinning effects of blood on nanofluid flow. The radiative blood flow affected by the suspended graphene nanoparticles in a blood vessel channel under the influences of magnetic field was investigated by [24]. The investigation revealed that significant temperature growth was observed due to the amplification of magnetic field. Fanelli *et al.,* [25] studied the application of external magnetic field for transporting the nanoparticles (drugs nanocarriers) through non-Newtonian blood flow. The study found that extra magnetic field strength was needed to absorb the certain number of nanoparticles in non-Newtonian blood compared to Newtonian blood. Based on the aforementioned study, all the blood flow were studied numerically, and no researcher was found analyzing the blood flow nature analytically. Therefore, this present study interested to concentrate the blood flow study on the side of analytical field.

Analytical solutions have several benefits. They help in validating numerical methods and understanding physical effects [26]. Analytical solutions are also useful in handling large-scale problems, such as hydrocarbon reservoirs, through dimensional analysis [27]. They provide fundamental building blocks for superposition of solutions in heat conduction problems [28]. Analytical solutions allow for efficient evaluation of exact solutions using short- and large-time representations [29]. They also provide a means to verify computer solutions obtained by numerical methods. For computational physicists, analytical solutions offer a way to resolve discrepancies between numerical simulations and experimental data, facilitating theory-simulation and theory-data comparisons. Nibedita Dash *et al.,* [30] developed a closed-form solution for the Navier-Stokes equations considering the Reiner-Rivlin constitutive relation for blood flow in a stenosed artery. Shabbir *et al.,* [31] conducted a theoretical analysis of blood flow in a tapered vascular tube with post-stenotic dilatation and arterial stenosis using the Herschel-Bulkley fluid model.

Magnetic fields have been found to have various effects on blood flow. In some cases, magnetic fields tend to accelerate blood flow velocity, which can be beneficial for improving blood circulation [32]. Additionally, magnetic fields have been shown to reduce blood viscosity, which can be used to control the blood flow rate [33]. The introduction of a magnetic field near a stenosis area in a blood vessel can alter the behaviour of blood flow, causing changes in velocity profiles and streamline patterns [34]. Furthermore, the application of external uniform magnetic fields has been studied to

determine their effect on blood flow in healthy and diseased cases. Overall, magnetic fields have the potential to influence blood flow characteristics and can be used for therapeutic purposes or to study the behaviour of blood flow in different scenarios. Hosseinzadeh *et al.,* [35] investigates the flow of non-Newtonian blood fluid with nanoparticles in a vessel with a porous wall, considering the effects of a magnetic field. An analytical study was conducted to investigate the hydrodynamic characteristics of non-Newtonian fluid flow in a rotating microchannel with a magnetic field [36]. Additionally, the impact of hybrid nanoparticles on peristaltic Maxwell blood flow in the presence of an induced magnetic field was analytically analyzed by [37], showing that hybrid nanoparticles exhibit superior heat transfer compared to copper nanoparticles in blood-based fluid. Gajbhiye *et al.,* [38] addressed the generalized Couette flow of immiscible fluids, including non-Newtonian fluids, between parallel plates under the presence of a magnetic field and electro-osmosis. Bilal *et al.,* [39] investigated analytically the use of blood as a viscoelastic fluid manipulated by an electromagnetic field, considering it as a Jeffrey fluid for nanoparticles (Ag and Al_2O_3) transport.

The porosity effect in blood flow refers to the influence of the presence of porous media on the flow characteristics of blood. Porous media can include materials such as atherosclerotic plaques or stents inserted in intracranial aneurysms [40]. The porosity of these materials affects the flow patterns, velocity distribution and shear forces experienced by the blood [41]. Studies have shown that decreasing porosity can lead to increased temperature heterogeneity, likelihood of vessel rupture and shear forces exerted on the vessel walls [42]. The use of low-porosity devices such as flow diverters, can significantly reduce flow parameters within aneurysm cavities [43]. The porosity effect is important to consider in understanding the behaviour of blood flow in various conditions, such as in the presence of diseases or during the treatment of intracranial aneurysms [44]. Blood flow analysis in channels with the effect of porosity has been studied analytically in several papers. Prakash *et al.,* [45] presented an analytical study on blood flow through a tapered porous channel driven by peristaltic pumping, considering thermal radiation effects and convective and slip boundary conditions. Rafaqat and Khan [46] investigated the compressible flow of viscous fluid in an asymmetric channel under peristalsis, incorporating the simultaneous effect of a magnetic field and flow through a porous medium. Reddy *et al.,* [47] studied the fluid flow in a parallel-plate channel partially filled with a porous medium, obtaining analytical solutions for velocity, flow rate and skin friction coefficient. Choudhari *et al.,* [48] investigated the role of hematocrit, slip and TPMA on blood flow in an axisymmetric inclined porous tube, obtaining closed-form solutions for velocity, flow rate and temperature. Yi *et al.,* [49] proposed a capillary bundle model to study the flow in porous media, deriving analytical expressions for tortuosity and permeability of Stokes flow through roughened capillaries.

The above review indicates that no analytical studies have been conducted to characterize blood rheology under the influence of magnetic fields and porosity, specifically utilizing the Casson fluid model and Laplace transformations for analytical solutions. This current analytical work addresses this gap by examining the effects of magnetic fields and porosity on blood flow within channel-shaped blood vessels. Additionally, it considers the impacts of nanoparticles, heat and mass transfer. By employing Laplace transformations to solve the unexplored Casson blood flow, this study fills important knowledge voids and offers a fresh perspective with wide-ranging biomedical applications. The research investigates the behaviour of Casson nanofluid mixed with blood, which exhibits differences compared to ordinary Newtonian fluids. The Casson fluid model employed in this study sheds new light on heat and mass transport, as well as fluid dynamics in blood flow scenarios. This analytical study involves simulating the governing equations of biofluid dynamics as linear partial differential equations (PDEs) and obtaining solutions using Laplace transformations. Employing Laplace transformations is beneficial for analyzing linear systems because it simplifies the differential

equation problems into algebraic ones, facilitating their resolution [50,51]. Laplace transformations serve as valuable tools across mathematics, physics, engineering and other disciplines, offering a method to solve differential equations and examine systems effectively.

2. Mathematical Formulation

In this study, the biofluid dynamics for blood flow moving along the blood vessel in the presence of cholesterol plaque and external magnetic field is simulated mathematically. Casson fluid model is used to describe the blood rheology and hence, this biofluid problem is governed by the momentum equation dealing with the Casson fluid model. The study investigates the flow behaviour of a Casson nanofluid with electrical conductivity in a channel, induced by a vertically moving plate located at $y = 0$, as illustrated in Figure 1, where its ideal model is depicted in Figure 2. This nanofluid comprises single-walled carbon nanotubes (SWCNTs) and multi-walled carbon nanotubes (MWCNTs) synthesized in human blood, flowing unsteadily through a porous medium while undergoing heat and mass transfer effects. The channel consists of two parallel walls separated by a distance h, and vertical plates extending infinitely upward along the x-axis, with their normals along the y-axis. A uniform transverse magnetic field B_0 is applied perpendicular to the x-axis. Initially, at $t = 0$, both the fluid and plates are stationary with constant temperature and concentration, denoted as T_h and C_h, respectively. Subsequently, at $t > 0$, the plate at $y = 0$ starts moving at a velocity U, raising the fluid's temperature and concentration to T_w and C_w, respectively, thereby enhancing the buoyancy force and initiating fluid motion in the x-direction *via* free convection. The channel walls extend infinitely, and all physical quantities solely depend on y and t. Under these assumptions and utilizing the Boussinesq approximation, the problem is described by the following PDEs Eq. (1) – (6)s.

$$\rho_{nf}\frac{\partial u(y,t)}{\partial t} = \mu_{nf}\left(1+\frac{1}{\beta}\right)\frac{\partial^2 u(y,t)}{\partial y^2} - \sigma_{nf}B_0^2 u(y,t) - \frac{\mu_{nf}}{k^*}u(y,t) + (\rho\beta_T)_{nf}g(T(y,t)-T_h) + (\rho\beta_C)_{nf}g(C(y,t)-C_h), \tag{1}$$

$$(\rho C_p)_{nf}\frac{\partial T(y,t)}{\partial t} = k_{nf}\frac{\partial^2 T(y,t)}{\partial y^2}, \tag{2}$$

$$\frac{\partial C(y,t)}{\partial t} = D_{nf}\frac{\partial^2 C(y,t)}{\partial y^2}, \tag{3}$$

coupled with the conditions for initial and boundary as

$$u(y,0) = 0, \quad T(y,0) = T_h, \quad C(y,0) = C_h; \quad \forall\, 0 \le y \le h, \tag{4}$$

$$u(0,t) = U, \quad T(0,t) = T_w, \quad C(0,t) = C_w; \quad \forall\, t > 0\,, \tag{5}$$

$$u(h,t) = 0, \quad T(h,t) = T_h, \quad C(h,t) = C_h; \quad \forall\, t > 0\,. \tag{6}$$

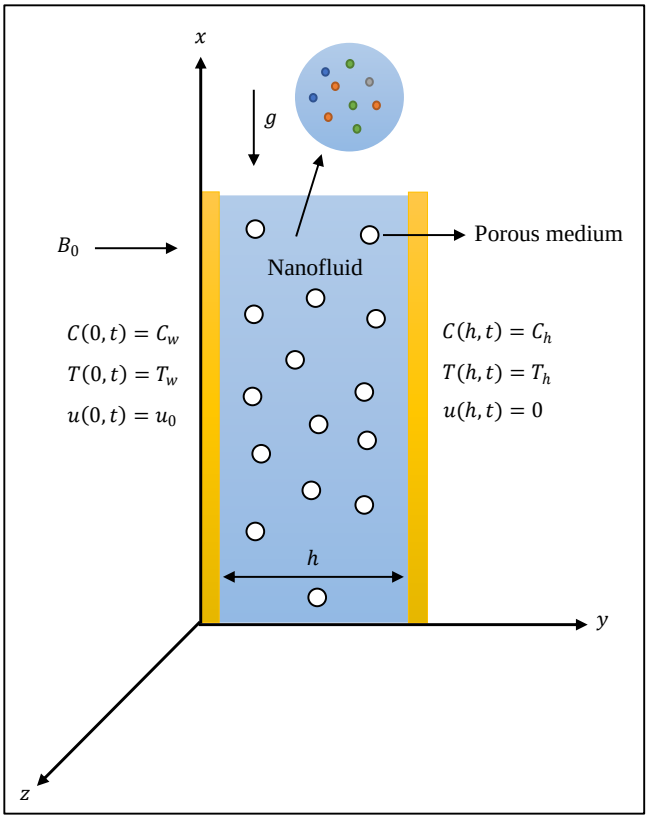

Fig. 1. Physical model for Casson nanofluid

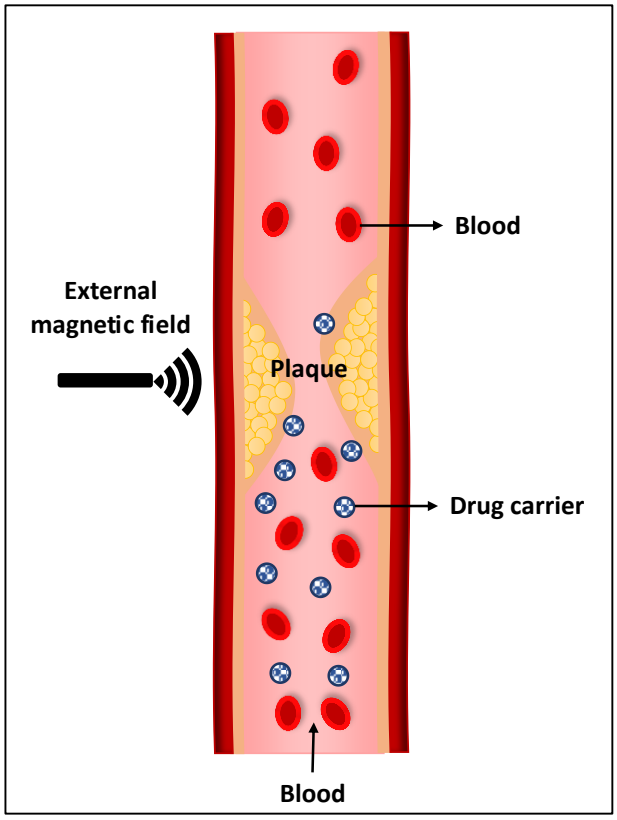

Fig. 2. Ideal model for blood flow

In the above equations, the correlation of nanofluid such as $\boldsymbol{\rho_{nf}}$: density, $\boldsymbol{\mu_{nf}}$: dynamic viscosity, $\boldsymbol{\sigma_{nf}}$: electric conductivity, $(\boldsymbol{\beta_T})_{\boldsymbol{nf}}$: thermal expansion coefficient, $(\boldsymbol{\beta_C})_{\boldsymbol{nf}}$: concentration expansion coefficient, $(\boldsymbol{C_p})_{\boldsymbol{nf}}$: specific heat, $\boldsymbol{k_{nf}}$: thermal conductivity and $\boldsymbol{D_{nf}}$: mass diffusivity are referred to nanofluid model proposed by Tiwari and Das [52], which respectively defines as,

$$\mu_{nf} = (1-\phi)\rho_f + \phi\rho_{CNTs}, \quad \mu_{nf} = \frac{\mu_f}{(1-\phi)^{2.5}},$$
$$\sigma_{nf} = 1 + \frac{3\left(\frac{\sigma_{CNTs}}{\sigma_f} - 1\right)\phi}{\left(\frac{\sigma_{CNTs}}{\sigma_f} + 2\right) - \phi\left(\frac{\sigma_{CNTs}}{\sigma_f} - 1\right)}, \quad \beta_{nf} = \frac{(1-\phi)(\rho\beta)_f + \phi(\rho\beta)_{CNTs}}{\rho_{nf}},$$
$$(C_p)_{nf} = \frac{(1-\phi)(\rho C_p)_f + \phi(\rho C_p)_{CNTs}}{\rho_{nf}}, \tag{7}$$
$$k_{nf} = \left(\frac{1-\phi+2\phi\frac{k_{CNTs}}{k_{CNTs}-k_f}\ln\frac{k_{CNTs}+k_f}{2k_f}}{1-\phi+2\phi\frac{k_f}{k_{CNTs}-k_f}ln\frac{k_{CNTs}+k_f}{2k_f}}\right)k_f, \quad D_{nf} = (1-\phi)D_f.$$

Additionally, the terms $\boldsymbol{\beta}$ indicates the Casson fluid parameter, $\boldsymbol{u(y,t)}$ is nanofluid velocity, $\boldsymbol{k^*}$ is porous medium permeability, $\boldsymbol{g}$ is acceleration due to gravity, $\boldsymbol{T(y,t)}$ is nanofluid temperature and $\boldsymbol{C(y,t)}$ is nanofluid concentration. The properties of nanoparticles and base fluid listed in Table 1 serve as the reference for the correlation presented in Eq. (7).

Table 1
Thermophysical properties of considered nanofluids

Substance/properties	SWCNTs	MWCNTs	Human blood
ρ $(\mathrm{Kgm^{-3}})$	2600	1600	1053
C_p $(\mathrm{JKg^{-1}K^{-1}})$	425	796	3594
k $(\mathrm{Wm^{-1}K^{-1}})$	6600	3000	0.492
σ $(\mathrm{Sm^{-1}})$	10^6 - 10^7	1.9×10^{-4}	0.8
$\beta \times 10^{-1}$ $(\mathrm{K^{-1}})$	27	44	0.18

Next, the following dimensionless variables are introduced as in Eq. (8),

$$u^* = \frac{u}{U}, \quad y^* = \frac{y}{h}, \quad t^* = \frac{tv_f}{h^2}, \quad T^* = \frac{T - T_h}{T_w - T_h}, \quad C^* = \frac{T - T_h}{T_w - T_h}, \tag{8}$$

and are substituted into Eq. (1) – (6) together with correlation (7) for the conversion to dimensionless form as (neglected the * sign)

$$\frac{\partial u(y,t)}{\partial t} = \frac{1}{b_5}\frac{\partial^2 u(y,t)}{\partial y^2} - b_2 M u(y,t) - \frac{b_1}{K}u(y,t) + b_3 GrT(y,t) + b_4 GmC(y,t), \tag{9}$$

$$\frac{\partial T(y,t)}{\partial t} = \frac{1}{a_1}\frac{\partial^2 T(y,t)}{\partial y^2}, \tag{10}$$

$$\frac{\partial C(y,t)}{\partial t} = \frac{1}{a_2}\frac{\partial^2 C(y,t)}{\partial y^2}, \tag{11}$$

$$u(y,0) = 0, \quad T(y,0) = 0, \quad C(y,0) = 0; \quad \forall\, 0 \le y \le 1, \tag{12}$$

$$u(0,t) = T(0,t) = C(0,t) = 1; \quad \forall\, t > 0\,, \tag{13}$$

$$u(1,t) = T(1,t) = C(1,t) = 0; \quad \forall\, t > 0\,, \tag{14}$$

where,

$$\begin{aligned} &a_1 = \frac{\Pr \phi_4}{\lambda}, \quad a_2 = \frac{Sc}{1-\phi}, \quad b_1 = \frac{\phi_1}{\phi_2}, \quad b_2 = \frac{\sigma}{\phi_2}, \quad b_3 = \frac{\phi_3}{\phi_2}, \quad b_4 = \frac{\phi_5}{\phi_2}, \\ &b_5 = \frac{1}{b_1}\left(\frac{\gamma}{\gamma+1}\right), \quad \phi_1 = \frac{1}{(1-\phi)^{2.5}}, \quad \phi_2 = (1-\phi) + \phi\frac{\rho_{CNTs}}{\rho_f}, \\ &\phi_3 = (1-\phi) + \phi\frac{(\rho\beta_T)_{CNTs}}{(\rho\beta_T)_f}, \quad \phi_4 = (1-\phi) + \phi\frac{(\rho C_p)_{CNTs}}{(\rho C_p)_f}, \end{aligned} \tag{15}$$

$$\phi_5 = (1-\phi) + \phi\frac{(\rho\beta_C)_{CNTs}}{(\rho\beta_C)_f}$$

are constant parameters. Performing the non-dimensionalizing process, Eq. (8) – (14) leads to the appearance of dimensionless parameters as in Eq. (16),

$$\begin{aligned}&\mathrm{Pr} = \frac{(\rho C_p)_f \nu_f}{k_f}, \quad Sc = \frac{\nu_f}{D_f}, \quad M = \frac{\sigma_f B_0^2 h^2}{\mu_f}, \quad K = \frac{k^*}{h^2}, \quad Gr = \frac{g(\beta_T)_f h^2 (T_w - T)}{U\nu_f},\\ &Gm = \frac{g(\beta_C)_f h^2 (C_w - C)}{U\nu_f},\end{aligned} \tag{16}$$

which are known as Prandtl number, Schmidt number, magnetic field, porosity, Grashof number and modified Grashof number.

3. Solution of the Problem

The Laplace transform is applied to Eq. (9) – (14), yielding the following equations,

$$\frac{d^2}{dy^2}\bar{u}(y,s) - \left(b_5 s + b_6 M + \frac{b_7}{K}\right)\bar{u}(y,s) = -b_8 Gr\bar{T}(y,s) - b_9 Gm\bar{C}(y,s), \tag{17}$$

$$\frac{d^2}{dy^2}\bar{T}(y,s) - a_1 s\bar{T}(y,s) = 0, \tag{18}$$

$$\frac{d^2}{dy^2}\bar{C}(y,s) - a_2 s\bar{C}(y,s) = 0, \tag{19}$$

$$\bar{u}(0,s) = \bar{T}(0,s) = \bar{C}(0,s) = \frac{1}{s}, \tag{20}$$

$$\bar{u}(1,s) = \bar{T}(1,s) = \bar{C}(1,s) = 0 \tag{21}$$

Eq. (17) – (19) are then resolved using the boundary conditions of (20) and (21). Eventually, the closed forms of the temperature, concentration and velocity are obtained as follows *via* inverse Laplace:

$$\begin{aligned}u(y,t) = &-u_{1a}(y,t) + u_{1b}(y,t) - u_{1c}(y,t) + u_{1d}(y,t) - u_{1e}(y,t) + u_{2a}(y,t)\\ &- u_{2b}(y,t) + u_{2c}(y,t) - u_{2d}(y,t) + u_{2e}(y,t) - u_{3a}(y,t) + u_{3b}(y,t)\\ &+ u_{4a}(y,t) - u_{4b}(y,t) - u_{5a}(y,t) + u_{5b}(y,t) + u_{6a}(y,t) - u_{6b}(y,t),\end{aligned} \tag{22}$$

$$T(y,t) = \sum_{n=0}^{\infty}\left[\mathrm{erfc}\left(\frac{(2n+y)\sqrt{a_1}}{2\sqrt{t}}\right) - \mathrm{erfc}\left(\frac{(2n+2-y)\sqrt{a_1}}{2\sqrt{t}}\right)\right], \tag{23}$$

$$C(y,t) = \sum_{n=0}^{\infty}\left[\operatorname{erfc}\left(\frac{(2n+y)\sqrt{a_2}}{2\sqrt{t}}\right) - \operatorname{erfc}\left(\frac{(2n+2-y)\sqrt{a_2}}{2\sqrt{t}}\right)\right], \tag{24}$$

with

$$\begin{aligned}
u_{1a}(y,t) &= \sum_{n=0}^{\infty}\left[\begin{matrix}\frac{1}{2}\exp\left(d_5\sqrt{b_{11}}\right)\operatorname{erfc}\left(\frac{d_5}{2\sqrt{t}}+\sqrt{b_{11}t}\right)+\\ \frac{1}{2}\exp\left(-d_5\sqrt{b_{11}}\right)\operatorname{erfc}\left(\frac{d_5}{2\sqrt{t}}-\sqrt{b_{11}t}\right)\end{matrix}\right]\\
u_{1b}(y,t) &= \sum_{n=0}^{\infty}\left[\begin{matrix}\frac{Gr_2}{2}\exp\left(d_5\sqrt{b_{11}}\right)\operatorname{erfc}\left(\frac{d_5}{2\sqrt{t}}+\sqrt{b_{11}t}\right)+\\ \frac{Gr_2}{2}\exp\left(-d_5\sqrt{b_{11}}\right)\operatorname{erfc}\left(\frac{d_5}{2\sqrt{t}}-\sqrt{b_{11}t}\right)\end{matrix}\right]\\
u_{1c}(y,t) &= \sum_{n=0}^{\infty}\left[\begin{matrix}\frac{Gr_2}{2}\exp\left(d_3t+d_5\sqrt{b_{11}+d_3}\right)\operatorname{erfc}\left(\frac{d_5}{2\sqrt{t}}+\sqrt{(b_{11}+d_3)t}\right)+\\ \frac{1}{2}\exp\left(d_3t-d_5\sqrt{b_{11}+d_3}\right)\operatorname{erfc}\left(\frac{d_5}{2\sqrt{t}}-\sqrt{(b_{11}+d_3)t}\right)\end{matrix}\right]\\
u_{1d}(y,t) &= \sum_{n=0}^{\infty}\left[\begin{matrix}\frac{Gm_2}{2}\exp\left(d_5\sqrt{b_{11}}\right)\operatorname{erfc}\left(\frac{d_5}{2\sqrt{t}}+\sqrt{b_{11}t}\right)+\\ \frac{Gm_2}{2}\exp\left(-d_5\sqrt{b_{11}}\right)\operatorname{erfc}\left(\frac{d_5}{2\sqrt{t}}-\sqrt{b_{11}t}\right)\end{matrix}\right]\\
u_{1e}(y,t) &= \sum_{n=0}^{\infty}\left[\begin{matrix}\frac{Gm_2}{2}\exp\left(d_4t+d_5\sqrt{b_{11}+d_4}\right)\operatorname{erfc}\left(\frac{d_5}{2\sqrt{t}}+\sqrt{(b_{11}+d_4)t}\right)+\\ \frac{Gm_2}{2}\exp\left(d_4t-d_5\sqrt{b_{11}+d_4}\right)\operatorname{erfc}\left(\frac{d_5}{2\sqrt{t}}-\sqrt{(b_{11}+d_4)t}\right)\end{matrix}\right]\\
u_{2a}(y,t) &= \sum_{n=0}^{\infty}\left[\begin{matrix}\frac{1}{2}\exp\left(d_6\sqrt{b_{11}}\right)\operatorname{erfc}\left(\frac{d_6}{2\sqrt{t}}+\sqrt{b_{11}t}\right)+\\ \frac{1}{2}\exp\left(-d_6\sqrt{b_{11}}\right)\operatorname{erfc}\left(\frac{d_6}{2\sqrt{t}}-\sqrt{b_{11}t}\right)\end{matrix}\right]\\
u_{2b}(y,t) &= \sum_{n=0}^{\infty}\left[\begin{matrix}\frac{Gr_2}{2}\exp\left(d_6\sqrt{b_{11}}\right)\operatorname{erfc}\left(\frac{d_6}{2\sqrt{t}}+\sqrt{b_{11}t}\right)+\\ \frac{Gr_2}{2}\exp\left(-d_6\sqrt{b_{11}}\right)\operatorname{erfc}\left(\frac{d_6}{2\sqrt{t}}-\sqrt{b_{11}t}\right)\end{matrix}\right]\\
u_{2c}(y,t) &= \sum_{n=0}^{\infty}\left[\begin{matrix}\frac{Gr_2}{2}\exp\left(d_3t+d_6\sqrt{b_{11}+d_3}\right)\operatorname{erfc}\left(\frac{d_6}{2\sqrt{t}}+\sqrt{(b_{11}+d_3)t}\right)+\\ \frac{1}{2}\exp\left(d_3t-d_6\sqrt{b_{11}+d_3}\right)\operatorname{erfc}\left(\frac{d_6}{2\sqrt{t}}-\sqrt{(b_{11}+d_3)t}\right)\end{matrix}\right]\\
u_{2d}(y,t) &= \sum_{n=0}^{\infty}\left[\begin{matrix}\frac{Gm_2}{2}\exp\left(d_6\sqrt{b_{11}}\right)\operatorname{erfc}\left(\frac{d_6}{2\sqrt{t}}+\sqrt{b_{11}t}\right)+\\ \frac{Gm_2}{2}\exp\left(-d_6\sqrt{b_{11}}\right)\operatorname{erfc}\left(\frac{d_6}{2\sqrt{t}}-\sqrt{b_{11}t}\right)\end{matrix}\right]
\end{aligned} \tag{25}$$

$$
\begin{aligned}
u_{2e}(y,t) &= \sum_{n=0}^{\infty}\left[\begin{array}{l}\frac{Gm_2}{2}\exp\left(d_4t+d_6\sqrt{b_{11}+d_4}\right)\operatorname{erfc}\left(\frac{d_6}{2\sqrt{t}}+\sqrt{(b_{11}+d_4)t}\right)+\\ \frac{Gm_2}{2}\exp\left(d_4t-d_6\sqrt{b_{11}+d_4}\right)\operatorname{erfc}\left(\frac{d_6}{2\sqrt{t}}-\sqrt{(b_{11}+d_4)t}\right)\end{array}\right]\\
u_{3a}(y,t) &= \sum_{n=0}^{\infty}\left[Gr_2\operatorname{erfc}\left(\frac{d_7}{2\sqrt{t}}\right)\right]\\
u_{3b}(y,t) &= \sum_{n=0}^{\infty}\left[\begin{array}{l}\frac{Gr_2}{2}\exp\left(d_3t+d_7\sqrt{d_3}\right)\operatorname{erfc}\left(\frac{d_7}{2\sqrt{t}}+\sqrt{d_3t}\right)+\\ \frac{Gr_2}{2}\exp\left(d_3t-d_7\sqrt{d_3}\right)\operatorname{erfc}\left(\frac{d_7}{2\sqrt{t}}-\sqrt{d_3t}\right)\end{array}\right]\\
u_{4a}(y,t) &= \sum_{n=0}^{\infty}\left[Gr_2 erfc\left(\frac{d_8}{2\sqrt{t}}\right)\right]\\
u_{4b}(y,t) &= \sum_{n=0}^{\infty}\left[\begin{array}{l}\frac{Gr_2}{2}\exp\left(d_3t+d_8\sqrt{d_3}\right)\operatorname{erfc}\left(\frac{d_8}{2\sqrt{t}}+\sqrt{d_3t}\right)+\\ \frac{Gr_2}{2}\exp\left(d_3t-d_8\sqrt{d_3}\right)\operatorname{erfc}\left(\frac{d_8}{2\sqrt{t}}-\sqrt{d_3t}\right)\end{array}\right]\\
u_{5a}(y,t) &= \sum_{n=0}^{\infty}\left[Gm_2\operatorname{erfc}\left(\frac{d_9}{2\sqrt{t}}\right)\right]\\
u_{5b}(y,t) &= \sum_{n=0}^{\infty}\left[\begin{array}{l}\frac{Gm_2}{2}\exp\left(d_4t+d_9\sqrt{d_4}\right)\operatorname{erfc}\left(\frac{d_9}{2\sqrt{t}}+\sqrt{d_4t}\right)+\\ \frac{Gm}{2}\exp\left(d_4t-d_9\sqrt{d_4}\right)\operatorname{erfc}\left(\frac{d_9}{2\sqrt{t}}-\sqrt{d_4t}\right)\end{array}\right]\\
u_{6a}(y,t) &= \sum_{n=0}^{\infty}\left[Gm_2\operatorname{erfc}\left(\frac{d_{10}}{2\sqrt{t}}\right)\right]\\
u_{6b}(y,t) &= \sum_{n=0}^{\infty}\left[\begin{array}{l}\frac{Gm_2}{2}\exp\left(d_4t+d_{10}\sqrt{d_4}\right)\operatorname{erfc}\left(\frac{d_{10}}{2\sqrt{t}}+\sqrt{d_4t}\right)+\\ \frac{Gm}{2}\exp\left(d_4t-d_{10}\sqrt{d_4}\right)\operatorname{erfc}\left(\frac{d_{10}}{2\sqrt{t}}-\sqrt{d_4t}\right)\end{array}\right]
\end{aligned}
\tag{26}
$$

The local Nusselt number (rate of heat transfer) ($\boldsymbol{Nu}$), Sherwood number ($\boldsymbol{Sh}$) and skin friction coefficient (friction drags) ($\boldsymbol{\tau}$) are defined as,

$$
\begin{aligned}
Nu &= -\frac{k_{nf}}{k_f}\left(\frac{\partial T}{\partial y}\right)\Big|_{y=0,1},\\
Sh &= -\frac{D_{nf}}{D_f}\left(\frac{\partial C}{\partial y}\right)\Big|_{y=0,1},\\
\tau &= \mu_{nf}\left(1+\frac{1}{\gamma}\right)\left(\frac{\partial u}{\partial y}\right)\Big|_{y=0,1}.
\end{aligned}
\tag{27}
$$

4. Results and Discussion

4.1 Effects on Blood Velocity

The present investigation and solution employ the Laplace transform approach to address the unsteady flow of Casson nanofluid in the presence of a magnetic field, porous media and heat and mass transfer effects. Eq. (20) – (22) are graphically represented using Mathcad software to facilitate a more thorough examination of their impacts on the velocity, temperature and concentration propagation. The numerical computation is carried out by setting the parameters to a chosen value such as $\phi = 0.02, \beta = 1.5, M = 2, K = 0.5, Gr = 3, Gm = 5, \Pr = 21, Sc = 0.22$ and $t = 0.2$. Casson fluid is the appropriate model to describe the characteristics of human blood, according to the study [53]. Thus, it is important to note that the Prandtl number of human blood, as adapted by [54,55], is 21, Pr = 21, which is relatively high in comparison to other common base fluids like water.

Figure 3 shows how the magnetic parameter *M* affects velocity. An increase in *M* is shown to cause the velocity field to decrease along the channel. This is due to the fact that the applied magnetic field acts against the flow by producing a drag-like force known as the Lorentz force. In fact, the Lorentz force produces a flow resistance in the fluid, which causes the velocity profiles inside the vessel to decelerate. By controlling the nanofluid velocity and causing nanoparticles to exit the domain more slowly, this retarding force can further uniformly distribute drug nanoparticles throughout the blood stream, improving the efficiency of drug delivery. Drug carrier targeted delivery efficiency is improved when the amount of magnetic force rises. To boost the targeting effectiveness of drug carrier at the plaque, the current cannot be increased indefinitely, though. The aforementioned factors, along with the plaque's sensitivity to the magnetic field and its orientation with respect to the heart, also restrict the use of an external magnetic field.

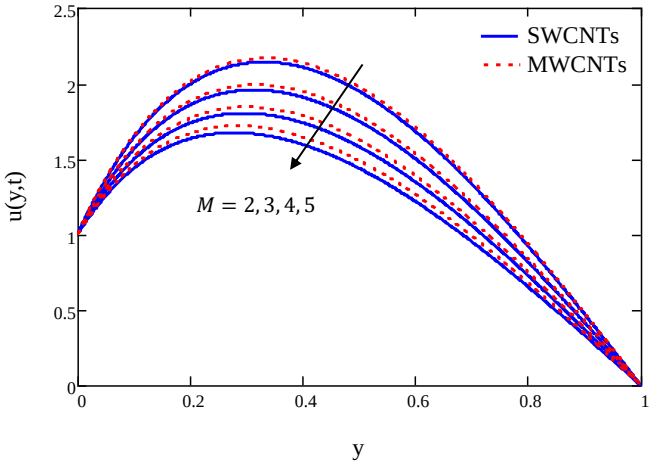

Fig. 3. Blood velocity with disparate values of M

Plaque porosity is a crucial component that varies as atherosclerosis disease progresses and with time. Reduced porosity makes the plaque stiffer and less noticeable when it comes to obstructing the flow. The consequence of reducing porosity is shown in Figure 4. Such that when the porosity level drops from 3.5 to 2.5, the blood velocity abruptly slows down due to the lowering plaque porosity. When the porosity level drops from 1.5 to 0.5, the plaque stiffens and hardens the arteries, which subsequently obstruct the blood flow.

Figure 5 shows that as the CNTs volume fraction rises, the resulting blood velocity increases. Eq. (1) shows that the blood velocity is dependent on both temperature and concentration, meaning that both factors will affect how quickly the blood velocity propagates. Because the intermolecular

interactions between nanoparticles lessen with temperature, the viscosity of blood decreases and hence accelerating the blood velocity in the vessels. The high velocity of blood flow can facilitate the transport of nanoparticles to regions of disturbed flow or areas with endothelial dysfunction, which are commonly associated with atherosclerotic plaque formation. Nanoparticles can accumulate in these regions through mechanisms such as margination, where they are pushed towards the vessel wall due to the shear forces exerted by flowing blood.

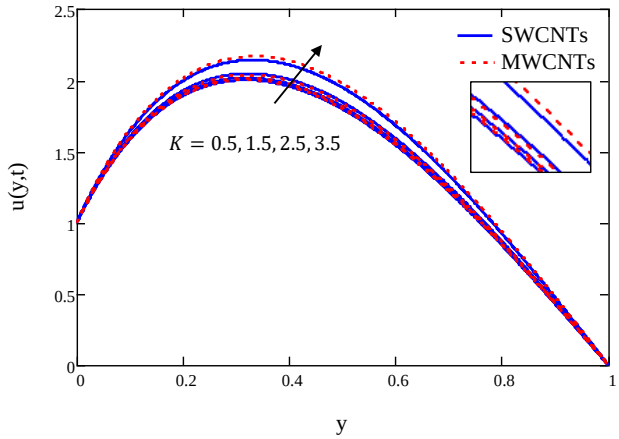

Fig. 4. Blood velocity with disparate values of K

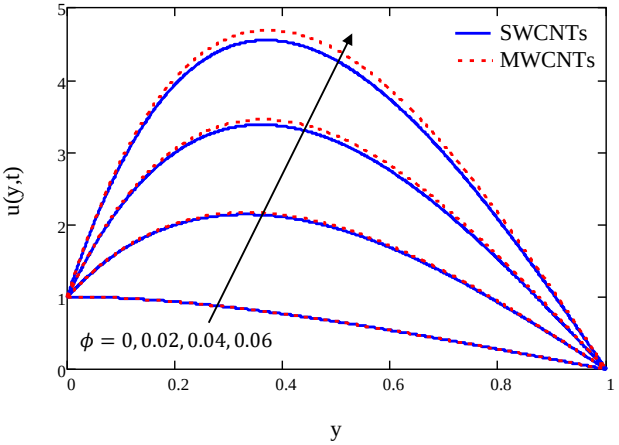

Fig. 5. Blood velocity with disparate values of ϕ

4.2 Effects on Blood Temperature

According to Figure 6, the heat transfer goes up gradually when the CNTs volume fraction is increased from 0 to 0.06. When treating atherosclerosis, temperature can be quite important, especially when using a nanoparticle-mediated hyperthermia strategy. These nanoparticles have the ability to selectively accumulate in atherosclerotic plaques and then activate them with external energy sources. This process is known as hyperthermia, which is the application of heat to targeted tissues. By softening the cholesterol deposits and improving the effectiveness of specific medications or procedures meant to remove plaque, these nanoparticles can aid in the breakdown of plaque in the arteries. Targeted ultrasound or thermal ablation are two methods that can be used to apply controlled heat to the injured areas.

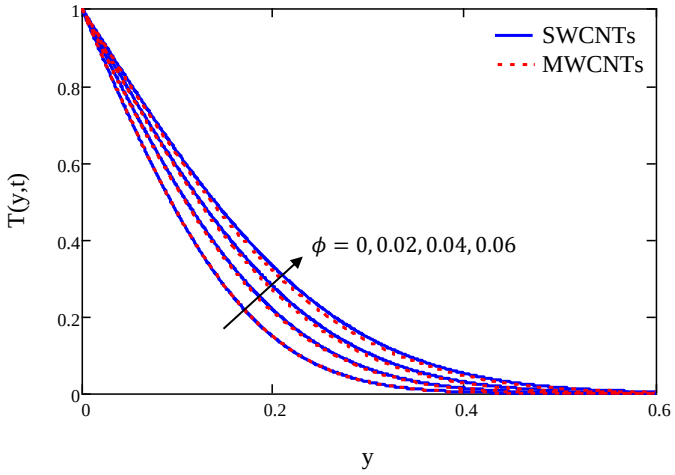

Fig. 6. Blood temperature with disparate values of ϕ

4.3 Effects on Blood Concentration

The mass transport describes the flow of blood-borne substances, such as oxygen and low-density lipoproteins, from the artery walls into the bloodstream or the other way around. According to theory suggested by Caro [56], the shear-dependent mass transfer of cholesterol between blood and the artery wall could be the cause of atherosclerosis. As a result, Figure 7 indicates that the concentration profile has marginally decreased due to the rising volume fraction of SWCNTs and MWCNTs, which will not exacerbate the atherosclerotic condition.

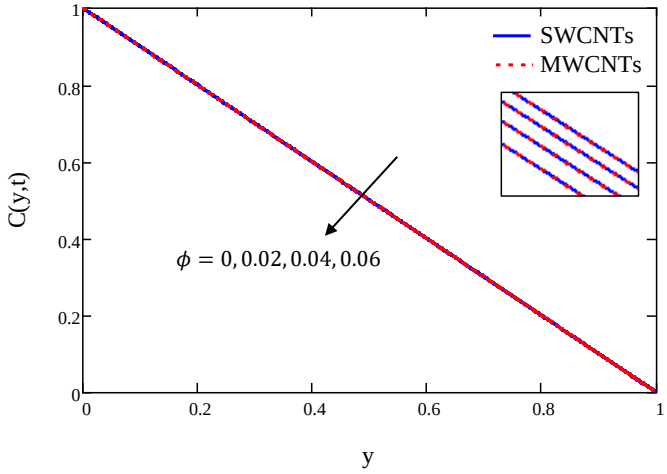

Fig. 7. Blood concentration with disparate values of ϕ

4.4 Effects on Skin Friction Coefficient, Nusselt Number and Sherwood Number

In bio-fluid dynamics, the shear stresses at the wall (skin friction coefficient) are a primary rheological measure that examine the force exerted by the fluid along a tangent to the artery's wall. Meanwhile, the Nusselt number (rate of heat transfer) is significant to characterize the convective heat transfer between a fluid and a solid surface and Sherwood number is evaluated to quantify convective mass transfer where its crucial in understanding the transport of substances such as oxygen, carbon dioxide, glucose or drugs across biological interfaces (blood vessel walls).

The impact of disparate values of magnetic field M, porosity K, and CNTs volume fraction on skin friction coefficient is evaluated and revealed in Table 2. It is noticed that the wall shear stress at $y =$

0 (τ_0) upsurges for both types of CNTs when the porosity level decreases. From the aforementioned results, it can infer that the reduced accumulation of cholesterol plaque causes the porosity level increase and any increase in fluid behavior reduce the wall shear stress marginally. However, at wall $y = 1$, the shear stress (τ_1) rises with the increase of porosity level. For the influence of magnetic field, the stress at wall ($y = 1$) goes up slowly by strengthening the magnetic field. Strong magnetic fields are known to elevate shear stress at the wall and raise flow resistance, which in turn causes an increase in skin friction within blood vessels. Opposite to stress at $y = 1$, the skin friction τ_0 drops with the magnetic field. Aside from that, the skin friction at $y = 1$ (τ_1) is significantly reduced by the rise in CNT volume fraction, and as a result, the blood flow indicates a low level of stress at blood vessels.

Table 3 displays the results of increasing CNTs volume fraction on the Nusselt number (rate of skin friction). There is an increased rate of heat transport for both walls (τ_0) and (τ_1) which is influenced by the increase in thermal conductivity when the volume percentage of CNTs increases. Based on Table 4, increasing the volume fraction of CNTs marginally increases the Sherwood number, which directly indicates to a quick transportation of mass between the blood and walls. These findings may suggest that the medications can swiftly reach the intended locations and improves the effectiveness of specific drugs or treatments meant to remove plaque.

Table 2
Variation of skin friction

M	K	ϕ	τ_0		τ_1	
			SWCNTs	MWCNTs	SWCNTs	MWCNTs
2	0.5	0.02	10.7839	10.8801	-8.9062	-8.9563
3	0.5	0.02	10.1665	10.3099	-8.5096	-8.5886
4	0.5	0.02	9.5793	9.7657	-8.1406	-8.2445
2	1.5	0.02	9.9745	10.0645	-8.3881	-8.4326
2	2.5	0.02	9.819	9.9078	-8.2902	-8.3337
2	0.5	0.04	23.8511	24.0835	-14.9015	-15.0263
2	0.5	0.06	37.5838	38.0218	-21.551	-21.7973

Table 3
Variation of Nusselt number

ϕ	Nu_0		Nu_1	
	SWCNTs	MWCNTs	SWCNTs	MWCNTs
0.02	2.9933	2.959	0.133	0.1195
0.04	3.3562	3.295	0.3543	0.308
0.06	3.6883	3.6046	0.6923	0.5973

Table 4
Variation of Sherwood number

ϕ	Sh_0		Sh_1	
	SWCNTs	MWCNTs	SWCNTs	MWCNTs
0.02	0.98	0.98	0.98	0.98
0.04	0.96	0.96	0.96	0.96
0.06	0.94	0.94	0.94	0.94

4.5 Comparison of SWCNTs and MWCNTs

According to nature of blood velocity in Figures 3 to 5, when contrasted to the use of SWCNTs, the low-density attribute of MWCNTs contributes to their noticeable profile. Additionally, MWCNTs tend to have thicker boundary layers, which promotes an increase in the velocity profile. Regarding

temperature in Figure 6, SWCNTs' exceptional thermal conductivity leads to their notable impact on temperature profiles and results for the rate of heat transfer. It should be noted that thermal conductivity describes a fluid's capacity to conduct and transfer heat, which suggests that a fluid with higher thermal conductivity will be able to conduct heat more effectively and at a faster rate. This explanation is adapted to prominent temperature by SWCNTs. It should be noted that the mass diffusivity factor, which is exclusively applicable to substances like fluids or gases and usually associates with the diffusion of molecules inside those substances, has a major impact on the concentration profile results. Because both CNTs are derived from human blood, marginal effect regarding concentration profiles have been noted.

5. Conclusions

The current work examines a blood flow model that takes into account the presence of atherosclerosis (porosity effect) in the blood arteries (channel geometry) and a magnetic field (an external source of energy). The Laplace transforms approach was used to solve the governing equations analytically. Mathcad-15 was extensively used to compute the data needed to convey the analysis's findings in tabular and graphical form. The distribution of velocity, temperature and concentration as well as wall shear stress, rate of heat transfer and mass transfer were investigated in relation to the effects of a magnetic field, porosity and CNT nanoparticles. The following is a summary of the significant findings from this study:

- Raising the values of the magnetic field parameter reduces the blood velocity distribution.
- Raising the values of porosity parameter and CNTs volume fraction accelerate the blood velocity distribution.
- Raising the values of CNTs volume fraction grows the blood temperature distribution and diminishes the blood concentration distribution.
- The rise of magnetic field parameter and thickness of boundary layer in the fluid flow model leads to the soaring of the shear stress encountered by the wall of blood at $y = 1$.
- The magnitude of shear stresses at the wall $y = 0$ is lessened by the increase in porosity level.
- The magnitude of shear stresses at the wall $y = 1$ is lessened by the increase in CNTs volume fraction.
- Raising the values of CNTs volume fraction increases the rate of heat transfer at both walls.

Given the intriguing findings obtained from present theoretical examination and practical use in clinical settings, it is expected that these insights could prove beneficial to healthcare professionals in predicting blood flow patterns within narrowed arteries. Furthermore, the collection of physical data from patients with atherosclerosis could hold significance for medical practitioners in determining appropriate treatment strategies.

Acknowledgement
This research was funded by Universiti Teknologi Malaysia under Matching Grant Scheme R.J130000.7354.4B748 and Q.J130000.3054.03M77.

References

[1] Sakakura, Kenichi, Masataka Nakano, Fumiyuki Otsuka, Elena Ladich, Frank D. Kolodgie, and Renu Virmani. "Pathophysiology of atherosclerosis plaque progression." *Heart, Lung and Circulation* 22, no. 6 (2013): 399-411. https://doi.org/10.1016/j.hlc.2013.03.001

[2] Björkegren, Johan LM, and Aldons J. Lusis. "Atherosclerosis: recent developments." *Cell* (2022). https://doi.org/10.1016/j.cell.2022.04.004

[3] Jebari-Benslaiman, Shifa, Unai Galicia-García, Asier Larrea-Sebal, Javier Rekondo Olaetxea, Iraide Alloza, Koen Vandenbroeck, Asier Benito-Vicente, and César Martín. "Pathophysiology of atherosclerosis." *International Journal of Molecular Sciences* 23, no. 6 (2022): 3346. https://doi.org/10.3390/ijms23063346

[4] Siddiqui, S. U., N. K. Verma, Shailesh Mishra, and R. S. Gupta. "Mathematical modelling of pulsatile flow of Casson's fluid in arterial stenosis." *Applied Mathematics and Computation* 210, no. 1 (2009): 1-10. https://doi.org/10.1016/j.amc.2007.05.070

[5] Pokhrel, Puskar R., Jeevan Kafle, Parameshwari Kattel, and Hari Prasad Gaire. "Analysis of blood flow through artery with mild stenosis." *Journal of Institute of Science and Technology* 25, no. 2 (2020): 33-38. https://doi.org/10.3126/jist.v25i2.33732

[6] Kafle, J., H. P. Gaire, P. R. Pokhrel, and P. Kattel. "Analysis of blood flow through curved artery with mild stenosis." *Mathematical Modeling and Computing* 9, no. 2 (2022): 217-225. https://doi.org/10.23939/mmc2022.02.217

[7] Kabir, Md Alamgir, Md Ferdous Alam, and Md Ashraf Uddin. "Numerical simulation of pulsatile blood flow: a study with normal artery, and arteries with single and multiple stenosis." *Journal of Engineering and Applied Science* 68 (2021): 1-15. https://doi.org/10.1186/s44147-021-00025-9

[8] Zidan, A. M., L. B. McCash, Salman Akhtar, Anber Saleem, Alibek Issakhov, and Sohail Nadeem. "Entropy generation for the blood flow in an artery with multiple stenosis having a catheter." *Alexandria Engineering Journal* 60, no. 6 (2021): 5741-5748. https://doi.org/10.1016/j.aej.2021.04.058

[9] Kamangar, Sarfaraz. "Numerical simulation of pulsatile blood flow characteristics in a multi stenosed coronary artery." *Bio-Medical Materials and Engineering* 32, no. 5 (2021): 309-321. https://doi.org/10.3233/BME-211234

[10] Achaba, Louiza, Mohamed Mahfouda, and Salah Benhadida. "Numerical study of the non-Newtonian blood flow in a stenosed artery using two rheological models." *Thermal Science* 20, no. 2 (2016): 449-460. https://doi.org/10.2298/TSCI130227161A

[11] Foong, Loke Kok, Majid Zarringhalam, Davood Toghraie, Niloufar Izadpanahi, Shu-Rong Yan, and Sara Rostami. "Numerical study for blood rheology inside an artery: The effects of stenosis and radius on the flow behavior." *Computer methods and programs in biomedicine* 193 (2020): 105457. https://doi.org/10.1016/j.cmpb.2020.105457

[12] Al-Azawy, Mohammed Ghalib, Saleem Khalefa Kadhim, and Azzam Sabah Hameed. "Newtonian and non-newtonian blood rheology inside a model of stenosis." *CFD Letters* 12, no. 11 (2020): 27-36. https://doi.org/10.37934/cfdl.12.11.2736

[13] Sinha, A., and G. C. Shit. "Modeling of blood flow in a constricted porous vessel under magnetic environment: an analytical approach." *International Journal of Applied and Computational Mathematics* 1 (2015): 219-234. https://doi.org/10.1007/s40819-014-0022-6

[14] Saleem, Anber, Salman Akhtar, Sohail Nadeem, Alibek Issakhov, and Mehdi Ghalambaz. "Blood flow through a catheterized artery having a mild stenosis at the wall with a blood clot at the centre." *Computer Modeling in Engineering & Sciences* 125, no. 2 (2020): 565-577. https://doi.org/10.32604/cmes.2020.011883

[15] Ismail, Zuhaila, Muhammad Sabaruddin Ahmad Jamali, Norliza Mohd Zain, and Lim Yeou Jiann. "Bioheat transfer of Blood Flow on Healthy and Unhealthy Bifurcated Artery: Stenosis." *Journal of Advanced Research in Applied Sciences and Engineering Technology* 28, no. 2 (2022): 56-79. https://doi.org/10.37934/araset.28.2.5679

[16] Mandal, Prashanta Kumar. "An unsteady analysis of non-Newtonian blood flow through tapered arteries with a stenosis." *International journal of non-linear mechanics* 40, no. 1 (2005): 151-164. https://doi.org/10.1016/j.ijnonlinmec.2004.07.007

[17] Wang, Xiaoping, Yanli Qiao, Haitao Qi, and Huanying Xu. "Numerical study of pulsatile non-Newtonian blood flow and heat transfer in small vessels under a magnetic field." *International Communications in Heat and Mass Transfer* 133 (2022): 105930. https://doi.org/10.1016/j.icheatmasstransfer.2022.105930

[18] Arjmandi, Hamidreza, Mohammad Zoofaghari, Seyed Vahid Rouzegar, Mladen Veletić, and Ilangko Balasingham. "On mathematical analysis of active drug transport coupled with flow-induced diffusion in blood vessels." *IEEE Transactions on NanoBioscience* 20, no. 1 (2020): 105-115. https://doi.org/10.1109/TNB.2020.3038635

[19] Abu-Hamdeh, Nidal H., Rashad AR Bantan, Farhad Aalizadeh, and Ashkan Alimoradi. "Controlled drug delivery using the magnetic nanoparticles in non-Newtonian blood vessels." *Alexandria Engineering Journal* 59, no. 6 (2020): 4049-4062. https://doi.org/10.1016/j.aej.2020.07.010

[20] Ali, Amjad, Attia Fatima, Zainab Bukhari, Hamayun Farooq, and Zaheer Abbas. "Non-Newtonian Casson pulsatile fluid flow influenced by Lorentz force in a porous channel with multiple constrictions: A numerical study." *Korea-Australia Rheology Journal* 33 (2021): 79-90. https://doi.org/10.1007/s13367-021-0007-z

[21] Tanveer, Anum, Mair Khan, T. Salahuddin, M. Y. Malik, and Farzana Khan. "Theoretical investigation of peristaltic activity in MHD based blood flow of non-Newtonian material." *Computer Methods and Programs in Biomedicine* 187 (2020): 105225. https://doi.org/10.1016/j.cmpb.2019.105225

[22] Ausaru, A., and P. Nagarani. "Effect of external body acceleration on solute dispersion in unsteady non-newtonian fluid flow-the generalized dispersion model approach." *International Journal of Applied and Computational Mathematics* 8 (2022): 1-21. https://doi.org/10.1007/s40819-021-01209-w

[23] Zaman, Akbar, and Ambreen Afsar Khan. "Time dependent non-Newtonian nano-fluid (blood) flow in w-shape stenosed channel; with curvature effects." *Mathematics and Computers in Simulation* 181 (2021): 82-97. https://doi.org/10.1016/j.matcom.2020.09.017

[24] Khazayinejad, Mehdi, Mohammad Hafezi, and Bahram Dabir. "Peristaltic transport of biological graphene-blood nanofluid considering inclined magnetic field and thermal radiation in a porous media." *Powder Technology* 384 (2021): 452-465. https://doi.org/10.1016/j.powtec.2021.02.036

[25] Fanelli, Claudia, Katerina Kaouri, Timothy N. Phillips, Timothy G. Myers, and Francesc Font. "Magnetic nanodrug delivery in non-Newtonian blood flows." *Microfluidics and Nanofluidics* 26, no. 10 (2022): 74. https://doi.org/10.1007/s10404-022-02576-6

[26] Sania, E., Seilabi. "Dimensional analysis and analytical solutions." (2023): 33-56. https://doi.org/10.1016/B978-0-323-90511-4.00002-2

[27] Woodbury, Keith A., Hamidreza Najafi, Filippo De Monte, and James V. Beck. "Inverse Heat Conduction: Ill-Posed Problems." (2023). https://doi.org/10.1002/9781119840220

[28] Kucheva, N. A. "Analytical solution of the problem of thermoelasticity for a plate heated by a source with a constant heat supply on one surface." *Turkish Journal of Computer and Mathematics Education (TURCOMAT)* 12, no. 10 (2021): 1622-1633.

[29] Kato, Sumio, and Shoichi Matsuda. "Analytical solution for the problem of one-dimensional quasi-steady non-charring ablation in a semi-infinite solid with temperature-dependent thermo-physical properties." *Thermal Science and Engineering Progress* 31 (2022): 101181. https://doi.org/10.1016/j.tsep.2021.101181

[30] Dash, Nibedita, and Sarita Singh. "Analytical study of non-Newtonian Reiner–Rivlin model for blood flow through tapered stenotic artery." *Математическая биология и биоинформатика* 15, no. 2 (2020): 295-312. https://doi.org/10.17537/2020.15.295

[31] Shabbir, Muhammad Shahzad, Nasir Ali, and Zaheer Abbas. "Impact of unsteadiness on the non-Newtonian flow of blood in a vascular tube with stenosis and aneurysm: analytical solution." *Waves in Random and Complex Media* (2023): 1-15. https://doi.org/10.1080/17455030.2023.2167018

[32] Bunonyo, K. W., and L. Ebiwareme. "Influence of a Magnetic Field on Blood Flow Through an Inclined Tapered Vessel with a Heat Source."

[33] Patel, Harshad, and Nilesh Patel. "Study of fractional-order model on Casson blood flow in stenosed artery with magnetic field effect." *Waves in Random and Complex Media* (2023): 1-19. https://doi.org/10.1080/17455030.2023.2185085

[34] Al-Griffi, Takia AJ, and Abdul-Sattar J. Al-Saif. "Modify homotopy perturbation method using yang transform to study the effect of magnetic field with mass and heat transfer on pulsatile blood flow in tapered stenosis arteries." *Heat Transfer* 52, no. 3 (2023): 2249-2276. https://doi.org/10.1002/htj.22783

[35] Hosseinzadeh, S., Kh Hosseinzadeh, A. Hasibi, and D. D. Ganji. "Hydrothermal analysis on non-Newtonian nanofluid flow of blood through porous vessels." *Proceedings of the Institution of Mechanical Engineers, Part E: Journal of Process Mechanical Engineering* 236, no. 4 (2022): 1604-1615. https://doi.org/10.1177/09544089211069211

[36] Siva, Thota, Srinivas Jangili, and Bidyasagar Kumbhakar. "A theoretical analysis of rotating electromagnetohydrodynamic and electroosmotic transport of couple stress fluid through a microchannel." (2023). https://doi.org/10.21203/rs.3.rs-3130856/v1

[37] Dolui, Soumini, Bivas Bhaumik, Soumen De, and Satyasaran Changdar. "EFFECT OF A VARIABLE MAGNETIC FIELD ON PERISTALTIC SLIP FLOW OF BLOOD-BASED HYBRID NANOFLUID THROUGH A NONUNIFORM ANNULAR CHANNEL." *Journal of Mechanics in Medicine and Biology* 23, no. 01 (2023): 2250070. https://doi.org/10.1142/S0219519422500701

[38] Gajbhiye, Sneha, Arundhati Warke, and Ramesh Katta. "Role of electromagnetic analysis in radiative immiscible Newtonian and non-Newtonian fluids through a microchannel with chemical reactions." *Heat Transfer* 51, no. 7 (2022): 6937-6960. https://doi.org/10.1002/htj.22631

[39] Bilal, Muhammad, Khurram Javid, and Nasir Ali. "Unsteady flow of hybrid fluid via peristaltic pumping in wavy micro-tube under electric and magnetic field effects: An application of Hall device and slip boundary." *Proceedings of the Institution of Mechanical Engineers, Part E: Journal of Process Mechanical Engineering* (2023): 09544089231157512. https://doi.org/10.1177/09544089231157512

[40] Alimohamadi, Haleh, Mohsen Imani, and Maedeh Shojaeizadeh. "Numerical simulation of porosity effect on blood flow pattern and atherosclerotic plaques temperature." *Int J Technol Enhance Emerg Eng Res* 2, no. 10 (2014): 44-49.

[41] Kumar, Anil. "Convective diffusion process of blood vessels in the presence of porous effects." *Acad. Open Internet J.* (2007): 21.

[42] Kumar, Anil. "Mathematical model of blood flow in arteries with porous effects." In *6th World Congress of Biomechanics (WCB 2010). August 1-6, 2010 Singapore: In Conjunction with 14th International Conference on Biomedical Engineering (ICBME) and 5th Asia Pacific Conference on Biomechanics (APBiomech)*, pp. 18-21. Springer Berlin Heidelberg, 2010.

[43] Augsburger, Luca, Mohamed Farhat, Philippe Reymond, Edouard Fonck, Zsolt Kulcsar, Nikos Stergiopulos, and Daniel Rüfenacht. "Effect of flow diverter porosity on intraaneurysmal blood flow." *Clinical Neuroradiology* 19, no. 3 (2009): 204-214. https://doi.org/10.1007/s00062-009-9005-0

[44] Al-Saad, Mohammed, Sana J. Yassen, Camilo Suarez-Afanador, Ahmed Kadhim AlShara, and Ali J. Chamkha. "Simulation of blood flow in human arteries as porous media." *Waves in Random and Complex Media* (2022): 1-11. https://doi.org/10.1080/17455030.2022.2162151

[45] Prakash, J., Dharmendra Tripathi, Abhishek Kumar Tiwari, Sadiq M. Sait, and Rahmat Ellahi. "Peristaltic pumping of nanofluids through a tapered channel in a porous environment: applications in blood flow." *Symmetry* 11, no. 7 (2019): 868. https://doi.org/10.3390/sym11070868

[46] Rafaqat, R., and A. A. Khan. "Effects of magnetic field and porosity on compressible flow in an asymmetric channel." *International Journal of Modern Physics B* (2023): 2450246. https://doi.org/10.1142/S0217979224502461

[47] Reddy, J. Sharath Kumar, and D. Bhargavi. "NUMERICAL STUDY OF FLUID FLOW IN A CHANNEL PARTIALLY FILLED WITH POROUS MEDIUM WITH DARCY− BRINKMAN− FORCHHEIMER EQUATION." *Special Topics & Reviews in Porous Media: An International Journal* 9, no. 4 (2018). https://doi.org/10.1615/SpecialTopicsRevPorousMedia.2018022123

[48] Choudhari, Rajashekhar, Manjunatha Gudekote, and Naveen Choudhari. "Analytical Solutions on the Flow of blood with the Effects of Hematocrit, Slip and TPMA in a porous tube." *Journal of Advanced Research in Fluid Mechanics and Thermal Sciences* 47, no. 1 (2018): 201-208.

[49] Yi, Shuang, Sheng Zheng, Shanshan Yang, and Guangrong Zhou. "Fractal Analysis of Stokes Flow in Tortuous Microchannels with Hydraulically Rough Surfaces." *Fractals* 30, no. 09 (2022): 2250166. https://doi.org/10.1142/S0218348X22501663

[50] Tölle, Johannes, Niklas Niemeyer, and Johannes Neugebauer. "Laplace-Transform GW." *arXiv preprint arXiv:2307.04508* (2023).

[51] Yadav, Dhiraj. "Utility of Laplace Transform in Mathematics." *International Journal of Advanced Engineering Research and Science* 10 (2023): 1. https://doi.org/10.22161/ijaers.101.7

[52] Tiwari, Raj Kamal, and Manab Kumar Das. "Heat transfer augmentation in a two-sided lid-driven differentially heated square cavity utilizing nanofluids." *International Journal of heat and Mass transfer* 50, no. 9-10 (2007): 2002-2018. https://doi.org/10.1016/j.ijheatmasstransfer.2006.09.034

[53] Noranuar, Wan Nura'in Nabilah, Ahmad Qushairi Mohamad, Sharidan Shafie, and Lim Yeou Jiann. "Heat and Mass Transfer on Magnetohydrodynamics Casson Carbon Nanotubes Nanofluid Flow in an Asymmetrical Channel via Porous Medium." *Symmetry* 15, no. 4 (2023): 946. https://doi.org/10.3390/sym15040946

[54] Noranuar, Wan Nura'in Nabilah, Ahmad Qushairi Mohamad, Sharidan Shafie, Ilyas Khan, Lim Yeou Jiann, and Mohd Rijal Ilias. "Non-coaxial rotation flow of MHD Casson nanofluid carbon nanotubes past a moving disk with porosity effect." *Ain Shams Engineering Journal* 12, no. 4 (2021): 4099-4110. https://doi.org/10.1016/j.asej.2021.03.011

[55] Saeed, Anwar, Abdelaziz Alsubie, Poom Kumam, Saleem Nasir, Taza Gul, and Wiyada Kumam. "Blood based hybrid nanofluid flow together with electromagnetic field and couple stresses." *Scientific Reports* 11, no. 1 (2021): 12865. https://doi.org/10.1038/s41598-021-92186-z

[56] Caro, Colin G. "Discovery of the role of wall shear in atherosclerosis." *Arteriosclerosis, thrombosis, and vascular biology* 29, no. 2 (2009): 158-161. https://doi.org/10.1161/ATVBAHA.108.166736